

Wind Driven Induction Generator Regulation Using Ant system Approach to Takagi Sugeno Fuzzy PID Control

A.H.Besheer¹

Electrical Engineering Department, Faculty of Engineering
University of Tabuk
P.O. Box 7031, Unit No. 1, Tabuk 47315-3470 KSA
abesheer@ut.edu.sa

Abstract: - This study introduces new tuning technique for the PID control scheme and its application to regulate the voltage magnitude and the frequency of wind energy conversion system (WECS). The developed technique is stem from blending the ant system optimization method with Takagi Sugeno (T-S) fuzzy system approach. The optimum relationship between the PID controller gains and the parameters of T-S fuzzy modules is explored using Ant system algorithm. A steady-state analysis for self excited slip ring induction generator is performed. The calculated and the experimental results on 1.1 KW laboratory machine enables the control characteristics to be deduced. Different simulation examples are provided to illustrate the effectiveness of the proposed technique. Finally, the response of a closed loop control scheme for WECS using chopper controlled external rotor resistance and fixed capacitor with thyristor controlled reactor shows that the proposed control approach exhibits a superior performance to that of established traditional control methods.

Key-Words: - T-S fuzzy control, PID control, Ant system optimization, WECS

1 Introduction

In the world of today there is a need for alternatives to the large coal and oil fired power plants. Renewable energy is one way to go, and in particular wind turbines have proven to be a solution [1]. The arrival of the new power devices technologies, new circuit topologies and novel control strategies are contributing to the success of the wind generation technology. A WECS can vary in size from a few hundred kilowatts to several megawatts. The size of the wind turbine largely determines the choice of the generator and converter system. Asynchronous generators are more common with systems up to 2MW, beyond which direct-driven permanent magnet synchronous machines are preferred [2][2]. In wind energy standalone generation systems, the frequency and the terminal voltage of the Self Excited Induction generators (SEIG) vary with load even when the rotor speed is maintained constant. The increase of the wind speed will lead to increase in the rotor speed that results in a commensurate increase in frequency, voltage and current. The use of slip-ring machine driven by a variable-speed turbine permits rotor slip-power control and when a grid connection is allowable the slip-ring machine may be operated as a double-output induction generator (DOIG) using the slip-energy recovery technique. In the case of SESRIG, the use of a simple rotor resistance controller leads to reduction of the system cost [3-4]. Since only a

capacitor bank needs to be connected to the stator terminals, the SESRIG provides a good quality ac source with little harmonic distortion to the stator load. Moreover, independent control of the voltage and frequency can be achieved easily. the generator frequency can be maintained reasonably constant - even with a wide variation in speed - by rotor resistance control, while the voltage can be controlled by varying the excitation capacitance.

PID controller is by far the most widely used control algorithm in the process industry, the performance of a PID controller, however, fully depends on the tuning of its parameters. Fuzzy control and tuning methodologies have emerged in last years as promising ways to approach nonlinear control problems and to deal with difficulties of conventional PID controllers [5][5]. The area of auto-tuning of PID controller using fuzzy systems has attracted many authors [6-8]. However, a common bottleneck encountered in fuzzy controller design is that derivation of fuzzy rules is often difficult and time-consuming, and relies on expert knowledge. To overcome this disadvantage, many automatic methods for fuzzy system design and optimization algorithms have been proposed, such as neural fuzzy systems [9][9][9] and evolutionary fuzzy systems [10][10].

One of the widely used methods for optimizing a fuzzy logic controller is to modify the rule base using this self-organizing algorithm automatically

¹ On leave from ESRI – Minoufiya University

according to previous responses until the desired control performance is achieved. Many works studied this problem such as [11], [10][12][12] and [13]. In [11], a tracking control problem is assumed to develop a self tuning PID control scheme with application to Antilock Braking System via combinations of fuzzy and genetic algorithms. While in [12], the approximation of analytical test function is performed using ant colony algorithm to tune the parameters of Takagi Sugeno (T-S) fuzzy rule base. The authors simplified their work by assuming constant consequence part instead of the ordinary linear function consequent part of T-S fuzzy system. In [13], Incremental fuzzy PID controller is used which is slightly different from the T-S fuzzy PID controller where, the scaling factors for input/output Macvicar-Whelan based fuzzy system are addressed in the ant colony optimization framework. In T-S fuzzy systems design, one challenging design task is the determination of the parameters of the consequent part.

Fuzzy PID is profusely applied to wind generation systems for the purpose of regulation and/or for capturing optimum power. In [14][14], a Mamdani type fuzzy logic control is used to tune the integral gain (K_i) of a PI controller to supervisory voltage/frequency control of a self-excited induction generator while in [15] an adaptive fuzzy proportional integral derivative control strategy to capture optimal power is presented. However, despite of the good results provided by all the aforementioned works, all have some common drawbacks that can be summarized in the following points:

- The behaviour of a FLC depends on shape of membership functions and the rule base.
- The design of the FLC was done according to the trial-and-error method rather than a guided approach.
- The presence of an expert knowledge is compulsory; conversely, in the absence of such knowledge, their design is usually slow and not optimized

Recently, the social inspired optimization algorithms become a successful alternative for the conventional tuning method to adapt the PID controllers. Using these new methods, the global optimal or suboptimal solutions of the optimized control scheme are found. These algorithms are adopted by many researchers for tuning PID controller in its classical and intelligent forms. One such approach is Ant System Optimization (ASO) which is founded on the foraging behavior of ants and their indirect communication based on pheromones; see for instance [16]. ASO has been applied to several combinatorial problems such as

job scheduling, routing optimization in data communication networks and telephone networks [17].

In this paper, ASO is employed to design the consequent part of a Takagi Sugeno fuzzy PI controller. The paper presents design procedures for a model free T-S fuzzy PI controller. Two independent T-S fuzzy systems are combined to tune different gains of PI controller. The optimum relationship between the PI controller parameters and the parameters of T-S fuzzy modules is explored. Using Ant system algorithm, the parameters of each T-S fuzzy system are optimally determined. The idea is to start with a tuned, conventional PI controller, replace it with an equivalent Takagi-Sugeno fuzzy PI controller and eventually fine-tune the T-S fuzzy tuner. This is relevant whenever a PI controller is possible or already implemented. In the proposed T-S Fuzzy Ant System PI, structure of T-S fuzzy system is well adapted via defining the optimum parameters of its consequence part. Once new rules are generated, the PI controller parameters are calculated from the defuzzification process. The developed technique extends our previous work in [16] to the case of WECS that presents interesting control demands and exhibits intrinsic non linear characteristics.

The key advantages for this paper are threefold:

- Developing a systematic approach to generate fuzzy rules from given input output data set by proposing T-S fuzzy module as a full optimizer for the PID controller instead of Mamdani fuzzy system [14] or a simplified T-S fuzzy module [12].
- Fine tune the consequent part of the ordinary T-S fuzzy system that is reported as a challenging design task [11][11-12].
- Explore the optimum relationship between the PID gains and the consequent part parameters of T-S fuzzy optimizer in highly nonlinear application without depend on prior knowledge base of the characteristics and response for the wind turbine system [14-15].

This paper has two main contributions. Firstly, a PI controller has been designed for WECS using a blending tuning mechanism namely Takagi – Sugeno fuzzy Ant system algorithm. Secondly, a satisfactory closed loop performance is achieved with respect to the conventional ZN frequency response tuning method. The objective of Ant System Optimization in this paper is to improve both the design efficiency of Takagi – Sugeno fuzzy systems and its performance to get optimal PI parameters. In this paper the voltage and frequency control of a three phase SESRIG is investigated by varying the external rotor resistance and the

excitation capacitance using the proposed Ant Takagi Sugeno Fuzzy PI controller.

This paper is organized as follows: section II demonstrates steady state model analysis of SESRIG that is considered as a main part of the proposed WECS. The control characteristic is deduced in section III by comparing the Experimental results to the calculated results with load and no load conditions. Specifically, the standalone WECS terminal output voltage and frequency control are shown in section IV. Takagi Sugeno fuzzy tuner for PI controller is presented in section V. Section VI introduces optimal parameter determination for Takagi Sugeno fuzzy systems using ant system optimization algorithm. Some simulation examples are provided to illustrate the effectiveness of the proposed technique in section VII. The proposed control strategy is applied to WECS in section VIII. Finally, a conclusion is set in section IX.

2 Analysis of SESRIG steady state model

In this section, the steady state model analysis of SESRIG that used in the proposed WECS control problem here is illustrated. Normalized equivalent circuit of SESRIG can be proposed as seen in Fig. 1 where the rotor resistance R_2 is the sum of the rotor winding resistance R_r and the external rotor resistance R_s , both referred to the stator side. The excitation capacitance is required for initiating voltage buildup and maintaining the output voltage. The circuit has been normalized to the base (rated) frequency through the introduction of the per-unit frequency a and the per-unit speed b [18][18][18]. The solution of the SEIG equivalent circuit have been developed using various methods. Among them, the nodal admittance method [19], is considered very simple and easy to follow, hence the following relationship may be established for successful voltage build-up:

$$E_1 (Y_t + Y_m + Y_2) = 0 \tag{1}$$

For a successful build-up air gap voltage E_1 can't be zero then:

$$Y_t + Y_m + Y_2 = 0 \tag{2}$$

With some mathematical manipulations and by equating the real and imaginary parts to zero, respectively, the following two equations in real numbers are obtained:

$$\frac{D_t R_t}{R_t^2 + X_t^2} + \frac{\frac{R_2}{a-b}}{\left(\frac{R_2}{a-b}\right)^2 + X_2^2} = zero \tag{3}$$

and

$$\frac{D_t X_t}{R_t^2 + X_t^2} - \frac{1}{X_m} - \frac{X_2}{\left(\frac{R_2}{a-b}\right)^2 + X_2^2} = zero \tag{4}$$

Where

$$D_t = \left(\frac{R_L}{a}\right)^2 + \left(X_L - \frac{X_C}{a^2}\right)^2 \tag{5}$$

$$R_t = \frac{R_L X_C^2}{a^5} + \frac{R_1}{a} \left[\left(\frac{R_L}{a}\right)^2 + \left(X_L - \frac{X_C}{a^2}\right)^2\right] \tag{6}$$

$$X_t = \left(\frac{R_L^2 X_C - X_L X_C^2}{a^4} + \frac{X_L^2 X_C}{a^2}\right) - X_1 \left[\left(\frac{R_L}{a}\right)^2 + \left(X_L - \frac{X_C}{a^2}\right)^2\right] \tag{7}$$

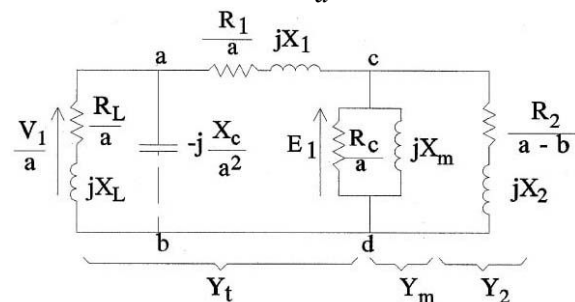


Fig. 1 Normalized equivalent circuit of Self Excited Slip Ring Induction Generator

Where a is per unit frequency (actual frequency/base frequency), b per-unit speed (rotor speed/synchronous speed) corresponding to base frequency, C excitation capacitance per phase, E_1 air-gap voltage per phase referred to base frequency, R_1 & R_2 stator and rotor winding resistances per phase. R_L stator load resistance per phase. V_1 Load voltage per phase, X_1 & X_2 Stator and rotor leakage reactance per phase, X_c Excitation capacitive reactance per phase and X_L Load reactance per phase. a and consequently X_m can be determined by iteratively solving (3) and (4). The magnetization curve (plot of E_1 versus X_m), enables E_1 to be determined and the equivalent circuit is completely solved [20]. For details on the parameters of the machine used see the Appendix.

3 Computed and Experimental Results

The main feature of the control characteristic for SESRIG used in standalone WECS is deduced in this section. For convenience, all of the machine parameters, except the excitation capacitance, are expressed in per unit. The effect of changing the external rotor resistance with constant excitation capacitance and vice versa on the output terminal voltage and frequency at load and no-load condition is presented. By the end of this section, the feasibility of the control method is confirmed by performing laboratory experiments on 1.1 KW

machine described in the Appendix. Fig. 2 shows the variation of the terminal voltage (V_T) against the rotor speed (b) at different values of excitation capacitance with zero external rotor resistance. At the same rotor speed, the voltage increases as the capacitance increases. Fig. 3 shows the variation of the output frequency (a) against the rotor speed (b) at different values of excitation capacitance with zero external rotor resistance. At the same rotor speed, changing the excitation capacitance has no effect on the frequency. Fig. 4 shows the variation of the terminal voltage (V_T) against the rotor speed (b) at different values of external rotor resistance and at excitation capacitance of 24 μF . At the same rotor speed, the voltage decreases as the rotor resistance increases. Fig. 5 shows the variation of the output frequency (a) against the rotor speed (b) at different values of external rotor resistance and at external capacitance of 24 μF . At the same rotor speed, the frequency decreases as the rotor resistance increases. Figs. (6-9) show the effect of changing the excitation capacitance with constant external rotor resistance and vice versa at loading conditions ($R_L = 8 \text{ p.u.}$) on the SESRIG output terminal voltage and frequency.

Remark 1:

- (1) It is obvious from Fig. 3 that, at no-load, the rated frequency (i.e. 1 p.u.) is almost occurred at the rated rotor speed.
- (2) Comparing (Fig. 6-7) to (Fig. 2-3) shows that loading causes a voltage and frequency drop from the no-load values.
- (3) Comparing (Fig.8-9) to (Fig.4-5) shows that the change caused by varying the external resistance in the loading case is much greater than the no-load case.
- (4) It is shown from (Fig. 2-5) that changing the excitation capacitance affects the voltage only, but changing the external resistance simultaneously changes the voltage and frequency.

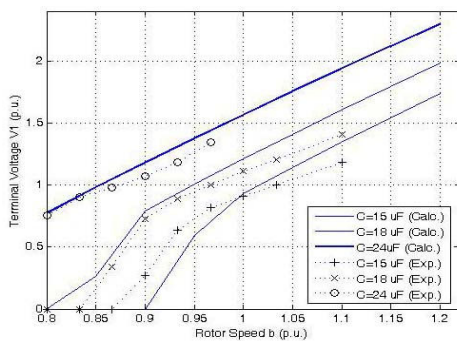


Fig. 2 Terminal Voltage (V_T) versus Rotor Speed (b) at different excitation capacitances at no load ($R_x=0$)

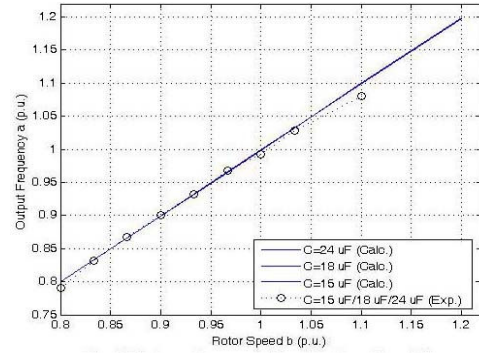


Fig. 3 Output Frequency (a) versus Rotor Speed (b) at different excitation capacitances at no load ($R_x=0$)

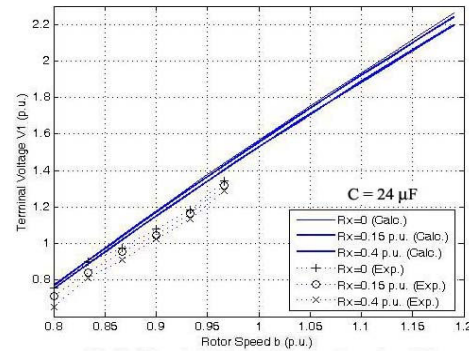


Fig. 4 Terminal Voltage (V_T) versus Rotor Speed (b) at different external resistance (R_x) at no load

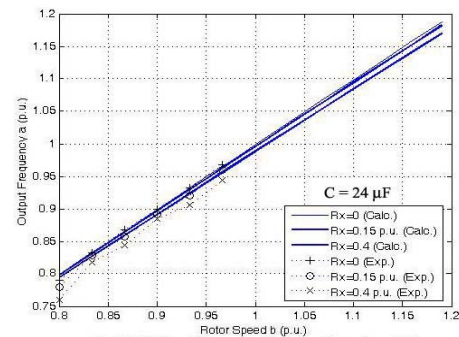


Fig. 5 Output Frequency (a) versus Rotor Speed (b) at different external resistance (R_x) at no load

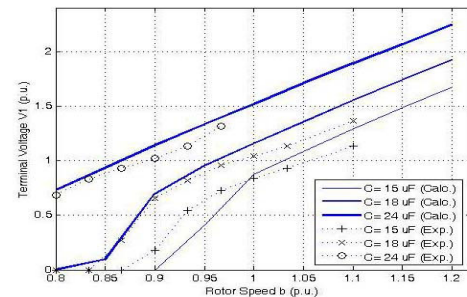


Fig. 6 Terminal Voltage (V_T) versus Rotor Speed (b) at different excitation capacitances at $R_L=8 \text{ p.u.}$ ($R_x=0$)

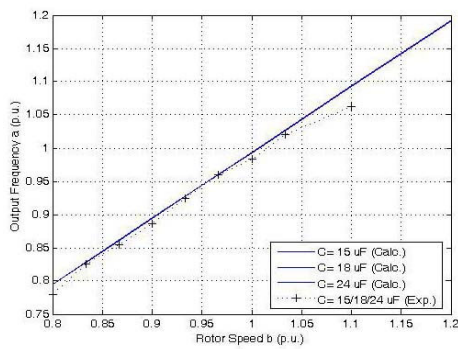


Fig. 7 Output Frequency (a) versus Rotor Speed (b) at different excitation capacitances at $R_L=8$ p.u. ($R_x=0$)

4 SESRIG Voltage and Frequency Control

From the previous characteristics, obtaining constant voltage and constant frequency output from the SESRIG used in standalone WECS is achievable by means of changing the excitation capacitor and the external rotor resistances simultaneously, as the rotor speed and the load vary. Fig. 10 shows that as the rotor speed (b) increase the external rotor resistance (R_x) required to maintain the frequency constant at 1 p.u. increases. It is noted that unity per-unit frequency is only achievable at rotor speeds above 1 p.u. Fig. 11 shows the corresponding terminal voltage. The terminal voltage (V_t) is constant as the rotor speed increases. At the same rotor speed, increasing the excitation capacitance increases the voltage. At a certain value of excitation capacitance, unity per-unit voltage can be obtained. For example, at rotor speed $b = 1.1$ p.u. and load resistance $R_L=8$ p.u., the external rotor resistance required to achieve $a = 1$ p.u. is 0.66 p.u. To keep the voltage at 1 p.u. at the same time, the external capacitance is adjusted to 16.11 μF . Fig. 12-13, show the external resistance and excitation capacitance needed to maintain nominal voltage and frequency at a constant rotor speeds (b) of 1.1 p.u. and 1.2 p.u. as the load current increases. For example, when rotor speed (b) is 1.1 and load current (I_L) is 0.25 p.u., the values of the external resistance and excitation capacitance which are needed to maintain the frequency and voltage at 1 p.u. are 0.7 p.u. and 16.55 μF respectively.

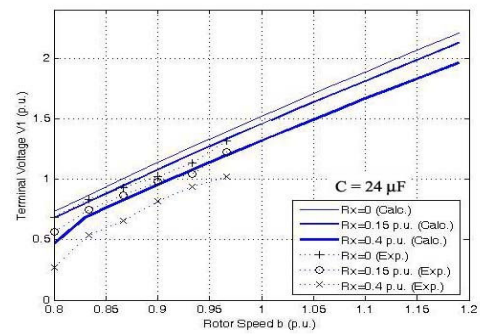


Fig. 8 Terminal Voltage (V_t) versus Rotor Speed (b) at different external resistance (R_x) at $R_L=8$ p.u.

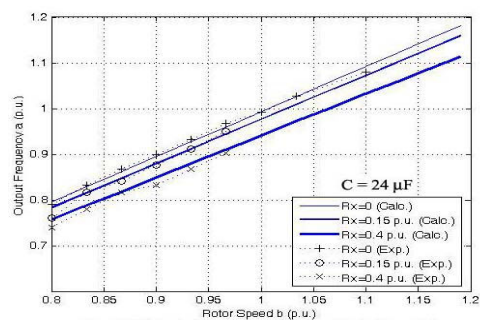


Fig. 9 Output Frequency (a) versus Rotor Speed (b) at different external resistance (R_x) at $R_L=8$ p.u.

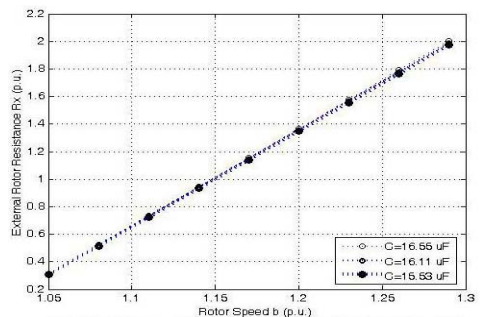


Fig. 10 External Rotor Resistance (R_x) required to maintain rated frequency as the rotor speed varies at different excitation capacitance ($R_L=8$)

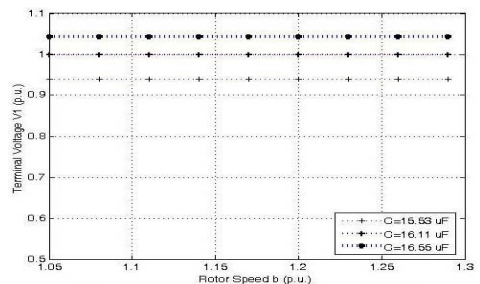


Fig. 11 Terminal voltage (V_t) at rated frequency as the rotor speed varies at different excitation capacitance ($R_L=8$)

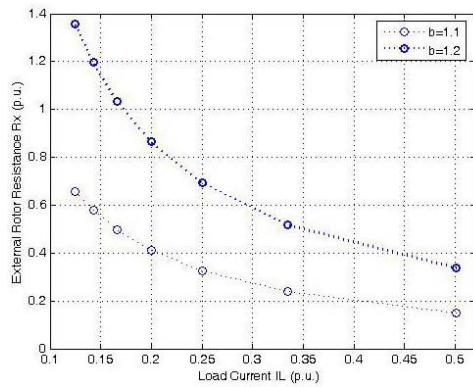


Fig. 12 Variation of external resistance (R_x) to operate at rated voltage and frequency as the load current increases

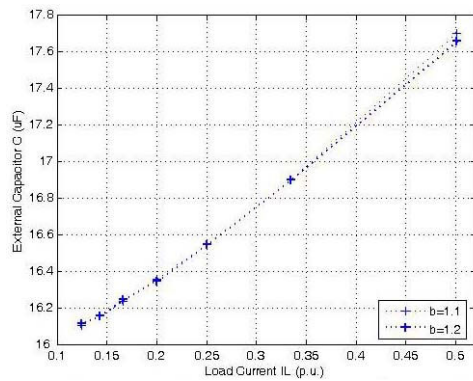


Fig. 13 Variation of excitation capacitance (C) to operate at rated voltage and frequency as the load current increases

Remark 2:

From the above figures and discussions in the last two sections, the following points can be concluded:

- (1) Comparison between the computed and experimental results reflects their close matching that reflects the adequateness of the circuit model and the solution method proposed in [20] and [21].
- (2) At constant load conditions, changing the external rotor resistance will affect the standalone WECS terminal output voltage and frequency while the excitation capacitance remains unchanged (i.e. increasing rotor speed (i.e. wind speed) should accompany with increasing the external rotor resistance while the excitation remains nearly constant)
- (3) At variable load conditions, simultaneous change in the external rotor resistance and the excitation capacitance is required in order to keep the standalone WECS working at the rated voltage and frequency (i.e. increasing the loading condition (the output power required from the standalone WECS) to be

delivered to the load) should accompany with decreasing the external rotor resistance and increasing the excitation capacitance).

5 T-S fuzzy Tuner for PID Controller

Many PID controllers were presented in literature, the expression of PID control law for a continuous time system is given as follows:

$$u(t) = K_p e(t) + \frac{K_p}{T_i} \int_0^t e(t) + K_p T_d \frac{de(t)}{dt} \quad (8)$$

where $e(t)$ is the error between the input and the output of the system; $u(t)$ is the control action generated by the PID controller; K_p is the proportional gain; T_i is the integral time constant; and T_d is the derivative time constant. In this section, three independent T-S fuzzy systems are used to tune different gains of PID controller. Each fuzzy module is assigned to obtain each PID gains. The typical T-S fuzzy systems studied in this paper have two inputs and one output. The input variables are error and rate of change of the error. We denote $e(t)$, $\dot{e}(t)$ and $y(t)$ as error, rate of change of error and system output, respectively. A fuzzy set for $e(t)$ (or $\dot{e}(t)$) is denoted as M (or L) and the corresponding membership is designated as $\mu_i(e(t))$ or $\mu_i(\dot{e}(t))$. Throughout this work, a Gaussians membership functions for the two inputs of the premise part of T-S fuzzy system are used. The error $e(t)$ and the rate of change of the error $\dot{e}(t)$ are normalized using three Gaussian membership functions; negative N , zero Z , and positive P , so that nine rules constitute the rule base for each module. For simplicity, the consequent part has been chosen to be a first order function of $e(t)$ and $\dot{e}(t)$. The rule bases have the following form:

Rule j : If $e(t)$ is M and $\dot{e}(t)$ is L then $k_i = a_{ij}e(t) + b_{ij}de(t)/dt$

Where $k_i = f(e(t), de(t)/dt)$ is the gain to be tuned, i.e. K_p, K_i or K_d . a_{ij} and b_{ij} are the constants, and $j=1, 2, \dots, 9$ is the rule number. In this paper, the weighted average technique is utilized to get the overall fuzzy output as follows:

Given a pair of $e(t), \dot{e}(t)$, the final output of the fuzzy system is inferred as follows [22]:

$$k^i = \frac{\sum_{j=1}^r w_j(e(t), \dot{e}(t))(a_{ij}e(t) + b_{ij}\dot{e}(t))}{\sum_{j=1}^r w_j(e(t), \dot{e}(t))} \quad (9)$$

$$w_j(e(t), \dot{e}(t)) = \prod_{j=1}^2 \mu_{A_j^i}(e(t), \dot{e}(t))$$

$$w_j(e(t), \dot{e}(t)) = \prod_{j=1}^2 \mu_{A_j^i}(e(t), \dot{e}(t))$$

Where

$\mu_{A_j}(e(t), \dot{e}(t))$ is the grade of membership of $(e(t), \dot{e}(t))$ in M and L . In this paper we assume that,

$w_j(e(t), de(t)/dt) \geq 0$ for $j=1,2,\dots,r$

$\sum_{j=1}^r w_j(e(t), \dot{e}(t)) > 0$ for all t . Therefore we obtain $h_j(e(t), \dot{e}(t)) \geq 0$ for $j=1,2,\dots,r$ and $\sum_{j=1}^r h_j(e(t), \dot{e}(t)) \geq 1$

Remark 3: Our approach is different from those of [11], [12] and [13] in the following ways.

- (1) A Takagi – Sugeno type of the fuzzy PID control system is assumed instead of incremental fuzzy PID control system.
- (2) The input membership functions of T-S fuzzy tuner are assumed to be constant (i.e. the membership function’s center “ c ” and its spread “ σ ” are constant over each rules and fuzzy system).
- (3) The total no. of free parameters to be tuned in is 117 parameters while in our proposed design procedures are 54 parameters (i.e. smaller computational burden).

6 ASO algorithm based T-S fuzzy optimal parameter determination

6.1 Ant System Optimization

The Ant System is the first member of a class of algorithms called Ant Colony Optimization (ACO) that was initially proposed by Colorni, Dorigo and Maniezzo[23]. This technique is adopted in this paper due to its simplicity. The main underlying idea, loosely inspired by the behavior of real ants, is that of a parallel search over several constructive computational threads based on local problem data and on a dynamic memory structure containing information on the quality of previously obtained result. In this algorithm, computational resources are allocated to a set of artificial ants that exploit a form of indirect communication mediated by the environment to find the shortest path from the ant nest to a set target. Ant algorithms have been proved to be a quick global optimal solution finder when compared to other heuristic methods such as simulated annealing and genetic algorithms. It also states that the ant algorithms have the quality to find

new optimal solution without reinitiating the computations from scratch.

6.2 T-S Fuzzy PID optimization problem

Usually, the optimization process consists of finding the controller parameters such as to minimize or maximize a given cost function of the closed loop system consisting of a fuzzy PID controller and an unknown plant. The optimization of step response of the system under control by minimizing a suitable performance criterion is the aim of this work. Each T-S fuzzy module consists of constant premise parameters (that is needn’t to be optimized) and 18 free consequence parameters (that will be optimized). The total number of free parameters to be optimized for the overall fuzzy system is 54. The AS algorithm is applied to optimize two different parameter matrices (A & B). These parameters matrices are driven by the consequence parts of fuzzy rule base. The dimension of both parameter matrices is “ 3×9 ”. The effectiveness of the proposed T-S Fuzzy controller is quantified by the following performance criteria that are evaluated at the end of a step response experiment. It includes the overshoot ζ , settling time t_s and steady state error e_{ss} of the system unit step response. The performance criterion of the system F is designed as follows:

$$F = \lambda_{\zeta} f_1 + \lambda_{t_s} f_2 + \lambda_{e_{ss}} f_3 \tag{10}$$

Where λ_{ζ} , λ_{t_s} and $\lambda_{e_{ss}}$ are three weighting coefficients and f_1, f_2 & f_3 are defined as follows:

$$f_1 = \zeta/\zeta_o, f_2 = t_s/t_{so} \text{ and } f_3 = \begin{cases} e_{ss}/e_{sso} & \text{if } e_{sso} \neq 0 \\ 0 & \text{if } e_{sso} = 0 \end{cases} \tag{11}$$

Where ζ_o , t_{so} and e_{sso} are the performance values obtained from ZN tuning formula. The parameters matrices for the problem of tuning T-S fuzzy PID controller are defined as:

$$A = \begin{bmatrix} a_{11} & \dots & a_{19} \\ \vdots & \ddots & \vdots \\ a_{31} & \dots & a_{39} \end{bmatrix} \text{ \& } B = \begin{bmatrix} b_{11} & \dots & b_{19} \\ \vdots & \ddots & \vdots \\ b_{31} & \dots & b_{39} \end{bmatrix} \tag{12}$$

Now, the control problem in this paper can be formulated as follows:

Given a plant $G(s)$ to be controlled (Fig.14), **determine** the optimum values of the parameters in (9) using ant system algorithm, hence, **find** the optimal PID parameters K_p , T_i and T_d **so that** the control system has the minimum value of given performance criterion “ F ” (10). Fig. 14 depicts the closed loop control system used in this paper.

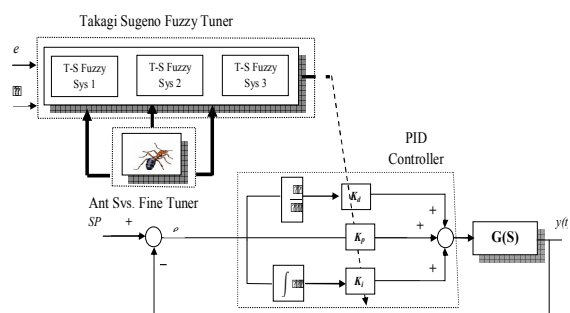


Fig. 14 The Proposed Closed loop Control System

We assume that the value of each parameter inside the matrices A & B has two digits; one digit before decimal point and the other after the decimal point. Using ant system optimization frame work a planar structure of 10 rows and 108 lines is adopted. 10 rows mean the number of $0 \leq 9$; 108 lines mean 108 bits of 54 parameters a_{ij} and b_{ij} . The nodes of lines $1 \leq 2 \leq 108$ is the 1st-2nd bit of a_{11} ; line $3 \leq 4 \leq 108$ is the 1st-2nd bit of b_{11} ; line $5 \leq 6 \leq 108$ is the 1st-2nd bit of a_{12} ; line $7 \leq 8 \leq 108$ is the 1st-2nd bit of b_{12} and so on till a_{39} & b_{39} . So, in the PID control AS, there are totally 1080 nodes. n_{ij} is used to denote the node j on line L_i . The y coordinate of the node n_{ij} is denoted by j . Let an ant depart from the origin O . In its each step forward, it chooses a node from the next line L_i ($i=1, 2, \dots, 108$) and then moves to this node along the straight line. When it moves to a node on line L_{108} , it completes one tour. Its moving path can be expressed as $\text{Path}=\{O, n_{1j_1}, n_{2j_2}, \dots, n_{108j_{108}}\}$. Obviously, the elements of A & B matrices represented by this path can be computed by the following for loop Matlab code:

```

k=1;
for i=1:3
for j=1:9
a(i,j)=path(1,k,m)+path(1,k+1,m)*1e-1;
b(i,j)=path(1,k+2,m)+path(1,k+3,m)*1e-1;
k=k+4;
end
end

```

(13)

where k is a dummy parameter and m is the total no. of ants.

6.3 Proposed Algorithm

Using the same technique used in [24][24] or the ant system optimization, we can modify the design algorithm presented in [13] to take into account the presence of T-S fuzzy system. The proposed AS Algorithm based T-S Fuzzy optimal PID parameter determination can be summarized as follows:

Step 1: Determine K_{po} , K_{io} and K_{do} using the classical Ziegler-Nichols tuning formula for a given

control system with a PID controller and compute the system's performance indexes ζ_o , t_{so} and e_{SSO} .

Step 2: Specify the initialization parameters of our proposed problem that contain the following:

- Values of α , β , ρ , τ_o and m .
- The maximum number of iterations t_{max} .
- A one-dimensional array $Path_k$ with 108 elements. Array $Path_k$ can be used to denote the moving path of ant k .

Step 3: Set the iteration counter $t=1$ and then place all of the m ants at the origin O .

Step 4: Set $i=1$.

Step 5: Set $k=1$.

Step 6: Compute the transition probability of each node on line L_i using the following formula

$$P_k(i, j, t) = \frac{\tau^\alpha(i, j, t) \eta^\beta(i, j, t)}{\sum_{j=0}^9 \tau^\alpha(i, j, t) \eta^\beta(i, j, t)}$$

Where $\eta(i, j, t)$ is the visibility of the node (i, j) and defined as $\eta(i, j, t) = 10 - |j - j^*| / 10$

Where the values of j^* are set in the following way:

- In the first iteration of the AS algorithm, the values of j^* ($i=1-108$, $j=0-9$) are assigned from the different values of the one dimensional array $Path_{k-initial}$.
- In each of the following iterations, j^* are determined from the calculated one dimensional array $Path_k$ (it contains different entities of matrices A & B) that is corresponding to optimal traveling path generated in the previous iteration by the ant

α, β represent respectively the relative importance of the pheromone concentration and visibility in transition probability

Step 7: Based on the calculated transition probability in the previous step and using Roulette wheel selection method, select a node on line L_i for ant k and move ant k to this node, then save the y coordinate of the node into the i^{th} element of $Path_k$.

Step 8: Set $k \leftarrow k+1$. If $k \leq m$, go to Step 6; Otherwise, continue.

Step 9: Set $i \leftarrow i+1$. If $i \leq 108$, go to Step 5; Otherwise, continue.

Step 10: For each ant k ($k=1, 2, \dots, m$): according to $Path_k$, compute different entities values of matrices A & B using formula (12).

Step 11: For each ant k ($k=1, 2, \dots, m$): evaluate the PID gain values from the T-S fuzzy system according to formula (9).

Step 12: For each ant k ($k=1, 2, \dots, m$): perform a simulation experiment using the calculated matrices A & B and compute the system's performance

indexes ζ^k, t_s^k and e_{ss}^k then compute the performance criterion F_k using formula (10).

Step 13: Compare all of the obtained F_k values and find the optimal ant path of this iteration ($Path_{k-optimal}$), that has minimum value of the performance criterion (i.e. $\min_k F_k, k=1,2,\dots,m$). Save the $Path_{k-optimal}$ and the corresponding optimal PID gains.

Step 14: Set each element of $Path_k$ to zero, $k=1, 2, \dots, m$.

Step 15: Update the pheromone concentration of each node on the moving ant path using the following updating rule:

$$\tau(i,j,t) = \rho\tau(i,j,t) + \Delta\tau(i,j)$$

$$\Delta\tau(i,j) = \sum_{k=1}^m \Delta\tau_k(i,j)$$

Where $0 < \rho < 1$ is the pheromone decay parameter $\Delta\tau_k(i,j)$ is the amount of pheromone laid at n_{ij} by ant k in the iteration just completed and computed by the following formula:

$$\Delta\tau_k(i,j) = \begin{cases} \frac{Q}{F_k} & \text{if ant } k \text{ passed through } n_{ij} \text{ in previous iter.} \\ 0 & \text{otherwise} \end{cases}$$

Where F_k is the value of performance criterion of ant k in the iteration just completed and computed by the formula (10); Q is a positive constant.

Step 16: Set $t \leftarrow t + 1$. If $t < t_{max}$ and all of the m ants do not make the same tour, place all the ants at the origin O and go to Step 4; if $t < t_{max}$ but all of the m ants make the same tour or $t = t_{max}$; stop.

7 Simulation Example

7.1. Validation simulation examples

Case 1 (High-Order System)

$$G_1(s) = \frac{1}{(1+s)(1+0.01s)(1+0.05s)(1+0.2s)}$$

Case 2 (Second Order System)

$$G_2(s) = \frac{1}{s^2 + 1.6s + 1}$$

Case 3 (Time delay System)

$$G_3(s) = \frac{ke^{-sL}}{1+Ts}, k = 0.1, L = 1.0, T = 5.0$$

A unit step experiment is performed on a closed loop control system that is consisted of $G(s)$ and T-S fuzzy PID controller for each case. This controller is tuned via Ant System algorithm. The parameters setting of the proposed algorithm are: $t_{max}=100, \rho=0.5, m=10, \alpha=3$ and $\beta=2$.

The unit step responses of the control system with the proposed Takagi Sugeno fuzzy ant system PID

controller (TSFASPID) are shown in Fig. 15-17 for all the cases. The control performance in these figures reflects the ability of the proposed control scheme in controlling different system. Hence, in the following section, it will be applied to the WECS which presents interesting control demands and exhibits intrinsic non linear characteristics.

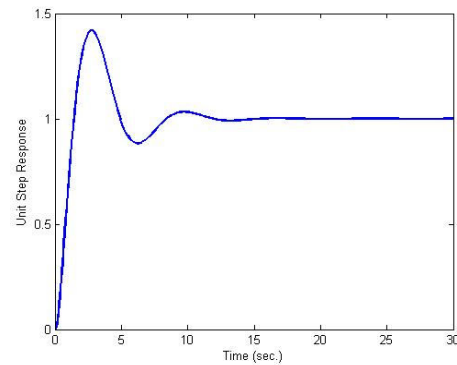


Fig. 15 The unit step response of the control system using ASTSFPID controller case (1)

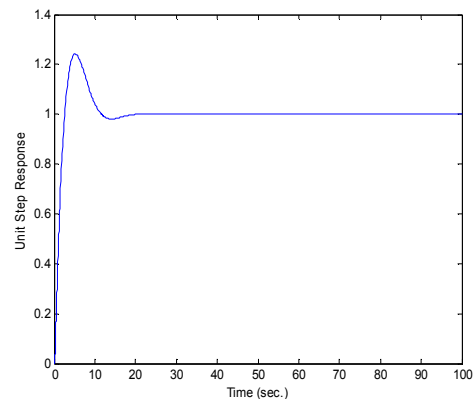


Fig. 16 The unit step response of the control system using ASTSFPID controller case (2)

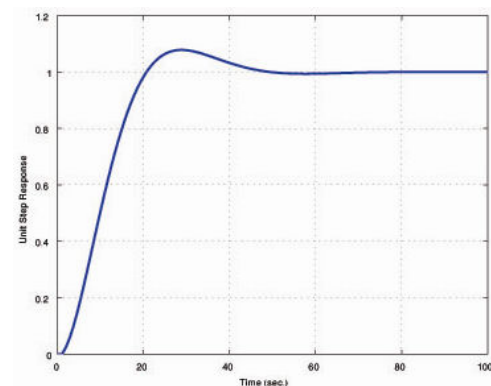


Fig. 17 The unit step response of the control system using ASTSFPID controller case (3)

7.2. Standalone WECS Simulation Using the Proposed Technique

In this section, the proposed technique is applied to the standalone WECS configured in Fig. 18 to automatically control the terminal output voltage and frequency of SESRIG when either the stator load impedance or the rotor speed changes. The goal is to keep the voltage and frequency at the value of 1 p.u. This is achieved by simultaneously changing the excitation capacitor and the added rotor resistance.

7.2.1. Chopper-controlled rotor external resistance

A chopper-controlled external resistance may be employed, as illustrated in Fig. 18. Rotor voltage is firstly rectified using an uncontrolled diode bridge rectifier. A chopper controlled resistance is connected on the dc output of the rectifier. Assuming that the diodes in the rotor bridge rectifier are ideal and the choke is lossless, the effective external resistance per phase in the rotor circuit, referred to the stator winding, is given by [25]:

$$R_x = 0.5n_m^2 (1-D)R_{DC} \quad (14)$$

As it can be inferred from (14), changing the duty cycle (D) of the chopper will result in changing the effective rotor resistance means that a variable external resistance is obtained in the rotor circuit.

7.2.2. Fixed capacitor-thyristor controlled reactor FC-TCR

The scheme shown in Fig.18 comprises a fixed excitation capacitor (FC) in parallel with a thyristor controlled reactor (TCR). The variation of the firing angle of the thyristor results in a variable leading VARs. The effective susceptance (B) per phase of such configuration is given by [26]:

$$B_e = \frac{2\alpha - \sin 2\alpha - \pi(2 - \frac{X_L}{X_C})}{\pi X_L} \quad (15)$$

7.2.3. Closed loop control

The stator terminal voltage and the output frequency are chosen as the feedback variable since any change in speed and stator load impedance will result in a corresponding change in the terminal voltage and output frequency. The stator terminal voltage signal is compared with the voltage reference signal. The voltage error signal is fed to a proportional-plus-integral (PI) controller that outputs a signal for the firing angle of the thyristor controlled inductor (TCR). The output frequency signal is compared with the frequency reference signal. The frequency error signal is fed to another PI controller that outputs a signal for the duty cycle of the chopper controlled resistance. Appropriate tuning of the PI controller is mandatory in order to give satisfactory dynamic performance of the proposed standalone WECS. Ziegler-Nichols (ZN) technique has been widely used among different traditional tuning methods. For this purpose, the SESRIG may be approximated as a first-

order system with the following transfer function [21][21]:

$$G(s) = \frac{ke^{-st_0}}{Ts+1} \quad (16)$$

where

K system gain

T time constant of the system

t_0 time delay of the system

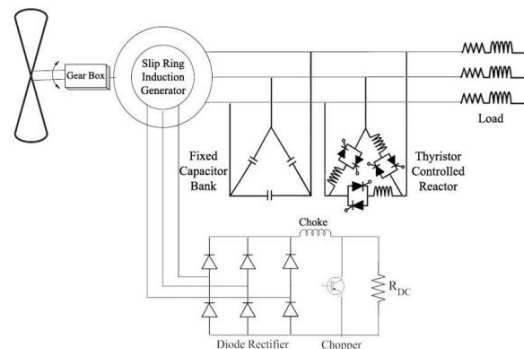


Fig. 18 Schematic Diagram for the system configuration

In our Matlab code expressing the proposed ant system based Takagi Seguno Fuzzy PI algorithm that introduced in section VI, the above transfer function and the gains of PI controller that concluded from ZN technique in [21][21] are used. The idea is to start the proposed algorithm with ZN PI gains then enhance the dynamic response of the closed loop system according to the performance index in (10) via the steps of the algorithm. Finally, the algorithm will reach to the optimal parameters of the PI controller that can be used in controlling the voltage and the frequency of the standalone WECS.

7.2.4. Closed Loop Control Simulation Results

This section contains the results of three simulation experiments using MATLAB/SIMULINK environment to study the dynamic response of SESRIG based standalone WECS with Takagi Seguno Fuzzy based Ant System PI closed loop control. For the sack of comparison, the results with ZN-PI controller designed in [21][21] are also presented. Firstly the response for changing the rotor speed (b) while the stator load resistance kept constant is presented. Secondly the response for changing the stator load resistance (R_L) while the rotor speed (b) kept constant is studied. Thirdly the response for changing the rotor speed (b) followed with a change in the stator load resistance (R_L) is introduced. Figs 19-24 show the dynamic response (output voltage and frequency) of the standalone WECS subjected to the proposed and traditional control method. The proposed PI controllers (ASTSFPI) after a short transient time restored both the output terminal voltage and frequency to the reference value (i.e. 1 p.u.) with reasonable overshoot and zero steady state error irrespective of changing the rotor speed and the stator load resistance. As seen from the following figures, the

proposed control method outperforms the traditional control method

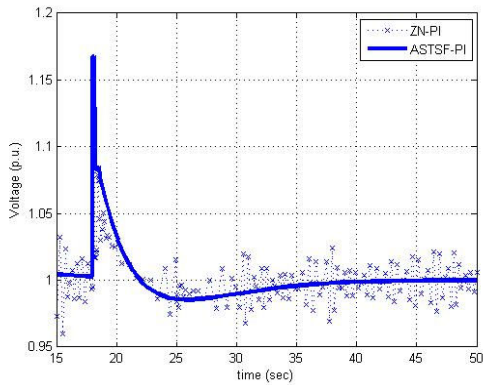


Fig. 19 Voltage Dynamic Response as b increases from 1.2 to 1.3 p.u. at $R_L=4$ p.u.

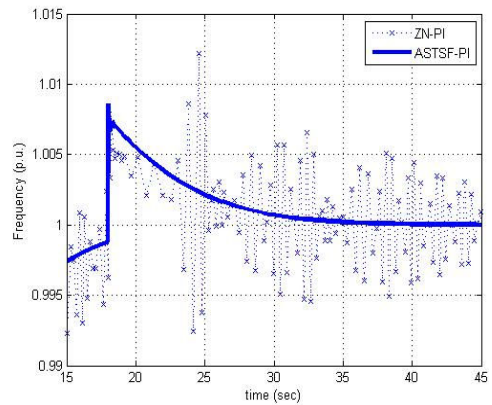


Fig.22 Frequency Dynamic Response as the load increases from 4 to 4.3 p.u. at $b=1.2$ p.u. with the proposed and the traditional control

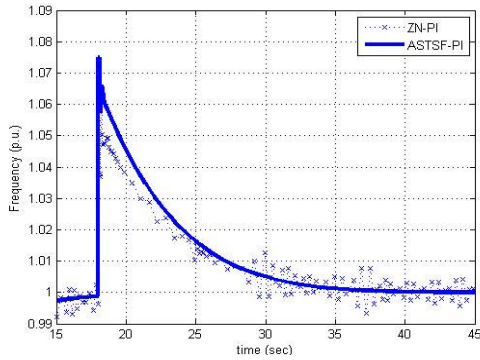


Fig. 20 Frequency Dynamic Response as b increases from 1.2 to 1.3 p.u. at $R_L=4$ p.u.

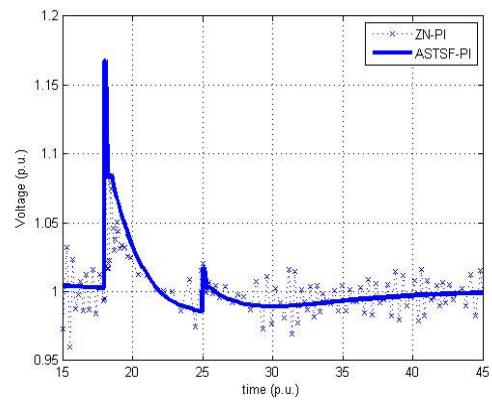


Fig. 23 Voltage Dynamic response as b & R_L change from $b=1.15$ to 1.3 p.u. and from $R_L=4.5$ to 4.3 p.u. with the proposed and the traditional control

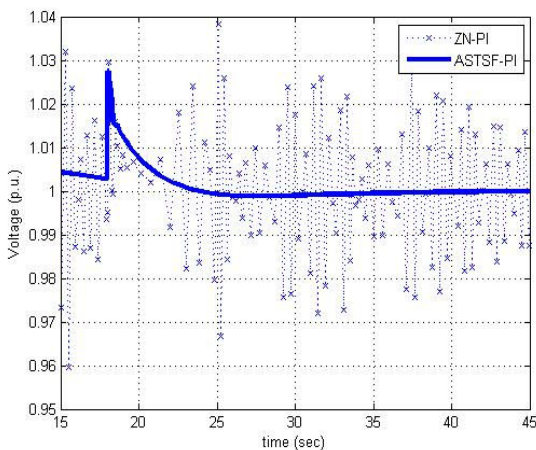


Fig. 21. voltage Dynamic Response as the load increases from 4 to 4.3 p.u. at $b=1.2$ p.u. with the proposed and the traditional control

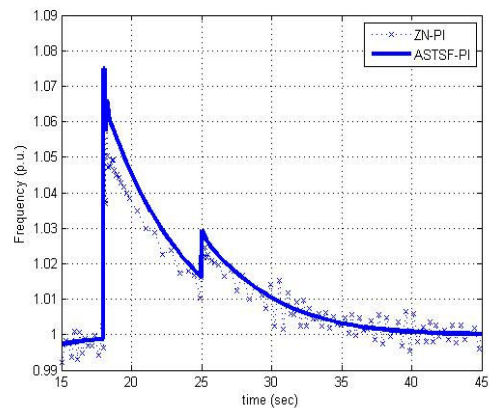


Fig. 24 Frequency Dynamic response as b & R_L change from $b=1.15$ to 1.3 p.u. and from $R_L=4.5$ to 4.3 p.u. with the proposed and the traditional control

Remarks 4:

- The proposed Ant colony tuning algorithm for the fuzzy PID scheme extends and develops the normal ant colony algorithm in [13&24] used to tune the PID controller scheme.
- The global optimal solution using the proposed algorithm is reached in less than 10 iterations offering fast convergence speed.
- The CPU time needed for obtaining the global optimal solution is approximately 5 seconds reflecting high computational efficiency.

8 Conclusion

In this paper, an optimal Takagi Seguno fuzzy PI controller is determined using ant system algorithm. The proposed controller is used to control the output voltage and frequency for standalone WECS at the sending end of self-excited slip-ring induction generator. The ant system algorithm search for the optimal parameters of the consequent part of the Takagi Seguno fuzzy system that is in turn produces the optimal PID gains. Steady-state performance and the control characteristics of the SESRIG have been obtained from an equivalent circuit analysis. It is shown that with varying rotor speed and load impedance both the frequency and the output voltage of the SESRIG can be maintained constant by rotor resistance control and excitation capacitance control over a wide range of speeds without exceeding the stator current limit. The proposed algorithm is easily implemented, has a good convergence property and has an efficient searching ability for the optimal PID controller. Computer simulation of closed-loop control for the WECS has also been described. It is shown that the proposed technique is very effective and useful for making the self excited induction generator feasible for remote windy areas.

Appendix

Performance analysis and experiments were conducted on a three-phase, two-pole, 50-Hz, 380-V, 2.2-A, 1.1-kW, star/star connected slip-ring induction machine whose per-unit equivalent circuit constants are $R_1=0.0511$, $X_1=0.0452$, $R_2=0.0413$, $X_2=0.0452$. The magnetization curve was represented by the following set of describing equations:

$$\begin{aligned} E_1 &= 2.5-0.7625 X_m & X_m < 2.1824 \\ E_1 &= 3.805-1.3769 X_m & 2.1824 \leq X_m < 2.3608 \end{aligned}$$

$$\begin{aligned} E_1 &= 13.1-5.3219 X_m & 2.3608 \leq X_m < 2.3941 \\ E_1 &= 7.36-2.9242 X_m & 2.3941 \leq X_m < 2.486 \\ E_1 &= 0 & X_m \geq 2.486 \end{aligned}$$

References:

- [1] J.F.Manwell, J.G. McGowan, A.L. Rogers, *Wind Energy Explained Theory, Design and Application*, John Wiley & sons LTD, England, 2002.
- [2] Rajib Datta and V. T. Ranganathan, "Variable-Speed Wind Power Generation Using Doubly Fed Wound Rotor Induction Machine—A Comparison With Alternative Schemes", *IEEE Transactions on Energy Conversion*, Vol.17, No. 3, September 2002, pp. 414 – 421.
- [3] A. A. Shaltout and A. F. El-Ramahi , " Maximum power tracking for a wind driven induction generator connected to a utility network", *Applied Energy*, Vol. 52, Issues 2-3, 1995, pp. 243-253.
- [4] Badrul H. Chowdhury and Srinivas Chellapilla, "Double-fed induction generator control for variable speed wind power generation", *Electric Power Systems Research*, Vol. 76, Issues 9-10, June 2006, pp. 786-800.
- [5] S.R.Vaishnav and Z.J.Khan, "Design and Performance of PID and Fuzzy Logic Controller with Smaller Rule Set for Higher Order System", *Proceedings of the World Congress on Engineering and Computer Science 2007*, San Francisco, USA, October 24-26, 2007.
- [6] Constantin Volosencu, "Control of Electrical Drives Based on Fuzzy Logic", *WSEAS Transactions on Systems and Control* Volume 3, Issue 9, September 2008, ISSN: 1991-8763.
- [7] SHIUH-JER HUANG and YI-HO LO, "Metal Chamber Temperature control by Using Fuzzy PID Gain Auto-tuning strategy", *WSEAS Transactions on Systems and Control*, Vol. 4, Issue 1, January 2009, ISSN: 1991-8763
- [8] Constantin Volosencu, "Stabilization of Fuzzy Control Systems", *WSEAS Transactions on Systems and Control*, Vol. 3, Issue 10, October 2008.
- [9] Lin, C.T. and Lee, C.S.G., "*Neural Fuzzy Systems: A Neural-Fuzzy Synergism to Intelligent Systems*", Englewood Cliffs: Prentice Hall, 1996.
- [10] Cordon, O., Herrera, F., Hoffmann, F. and Magdalena, L., "Genetic Fuzzy Systems: Evolutionary Tuning and Learning of Fuzzy Knowledge Bases" (Singapore: World Scientific), 2001.
- [11] Abdel Badie Sharkawy, "Genetic fuzzy self tuning PID controllers for antilock braking

- systems", *Alexandria Engineering Journal*, Vol. 45, No. 6, 2006, pp. 657-673.
- [12] Hadi Nobahari, Seid H. Pourtakdoust, "Optimization of fuzzy rule bases using continuous ant colony system", *Proceeding of the first International Conference on Modeling, Simulation and Applied optimization*, Sharjah, U.A.E, February 1-3, 2005.
- [13] Tan Guan-zheng and Dou Hong-quan, "ACS algorithm-based adaptive fuzzy PID controller and its application to CIP-I intelligent leg", *J.Cent. South Univ. Technol.* (2007)04-0528-09, Springer, DOI:10.1007/s11771-007-0103-3.
- [14] Hussein F. Soliman, Abdel-Fattah Attia, S. M. Mokhymar, M. A. L. Badr, "Fuzzy Algorithm for Supervisory Voltage/Frequency Control of a Self Excited Induction Generator", *Acta Polytechnica* Vol. 46 No. 6, 2006.
- [15] Kong Yigang and Wang Zhixin, "Optimal Power Capturing of Multi-MW Wind Generation System", *WSEAS Transactions on Systems* Issue 3, Volume 7, March 2008.
- [16] A.H.Besheer, "Tuning Method for PID Control Scheme:A blended Ant System Optimization Technique with Takagi Sugeno Fuzzy System", *ICFC 2010 - International Conference on Fuzzy Computation*, Valencia, Spain 24-26 October 2010.
- [17] Karl O. Jones, André Bouffet' "COMPARISON OF ANT COLONY OPTIMISATION AND DIFFERENTIAL EVOLUTION", *International Conference on Computer Systems and Technologies - CompSysTech'07*, 2007.
- [18] M. G. Say, *Alternating Current Machines*, 5th ed. London, U.K.: Pitman Publishers (ELBS), 1983.
- [19] T.F.Chan, "Analysis of self excited induction generators using an iterative method", *IEEE Transaction on Energy Conversion*, Vol. 10, No. 3, September 1995.
- [20] T. F. Chan, " Steady State Analysis of Self Excited Induction generators", *IEEE Transactions on Energy Conversion*, Vol. 9, No. 2, June 1994.
- [21] T. F. Chan, K. A. Nigim, and L. L. Lai, "Voltage and Frequency Control of Self-Excited Slip-Ring Induction Generators", *IEEE Transactions on Energy Conversion*, vol. 19, No. 1, March 2004.
- [22] A.H.Besheer and H.R.Emara "Relaxed LMI Based designs for Takagi Sugeno Fuzzy Regulators and Observers; Poly-Quadratic Lyapunov Function approach", *Proceedings of the 2009 IEEE International Conference on Systems, Man, and Cybernetics*, San Antonio, TX, USA - October 2009.
- [23] DORIGO M, V. Maniezzo and A. Colomi, "Ant system:nOptimization by a colony of cooperating agents", *IEEE Transaction on Systems Man and cybernetics – part B*, 26 (1), 1996, pp. 29-41.
- [24] Guanzheng Tan, Qingdong Zeng, Shengjun He and Guangchao,"Adaptive and robust design for PID controller based on ant system algorithm",*Advances in Natural Computation, Lecture Notes in Computer Science*,Vol 3612/2005, 2005, 915- 24, DOI:10.1007/11539902_113
- [25] Muhammad H. Rashid , *Power Electronics: Circuits, Devices and Applications*, Newyork, USA: Prentice Hall PTR, 2003.
- [26] Claudio A. Canizares, "Power Flow and Transient Stability Models of FACTS Controllers for Voltage and Angle Stability Studies", *IEEE Power Engineering Society Winter Meeting*, Vol. 2, Issue , 2000, pp. 1447 – 1454.